

## Liquid-tin-jet laser-plasma extreme ultraviolet generation

P. A. C. Jansson,<sup>a)</sup> B. A. M. Hansson, O. Hemberg, M. Otendal, A. Holmberg, J. de Groot, and H. M. Hertz

*Biomedical and X-Ray Physics, Royal Institute of Technology/Albanova, SE-106 91 Stockholm, Sweden*

(Received 18 November 2003; accepted 3 February 2004)

We demonstrate the applicability of liquid-metal jets in vacuum as regenerative targets for laser-plasma generation of extreme ultraviolet (EUV) and soft x-ray radiation. This extends the operation of liquid-jet laser-plasma sources to high-temperature, high- $Z$ , high-density, low-vapor-pressure materials with new spectral signatures. The system is demonstrated using tin (Sn) as the target due to its strong emission around  $\lambda \approx 13$  nm, which makes the material suitable for EUV lithography. We show a conversion efficiency of 2.5% into ( $2\% \text{ BW} \times 2\pi \times \text{sr}$ ) and report quantitative measurements of the ionic/atomic as well as particulate debris emission. © 2004 American Institute of Physics. [DOI: 10.1063/1.1690874]

Laser plasmas based on liquid-jet targets are gaining increasing importance as compact extreme ultraviolet (EUV) and soft x-ray sources. To date, predominantly low- $Z$  liquids and/or liquified inert gases have been employed as target materials for laser plasmas emitting in the 0.1 to a few keV range. In this letter we introduce moderate-melting-point metals as target liquids, thereby extending liquid-jet EUV/soft x-ray laser-plasma operation to new materials with new spectral signatures. As an example we use tin, motivated by its current interest for EUV lithography due its strong emission at  $\lambda \approx 13$  nm.

Laser plasmas are attractive compact x-ray and EUV sources due to their small size, high brightness and/or high flux, and high spatial stability. However, laser plasmas with conventional solid targets are of limited use for applications due to the production of debris and their limited operating time. Regenerative targets based on liquid droplets<sup>1</sup> or liquid jets<sup>2</sup> provide fresh target material at high density for all-day operation without interrupts and allow the use of high-repetition-rate lasers, thereby having potential for high average power. Furthermore, deposition of debris is significantly reduced.<sup>3</sup> By choosing a suitable target liquid and correct plasma conditions, the emission wavelength may be spectrally tailored to suit different applications, e.g., the extreme ultraviolet (e.g., water<sup>4,5</sup> and xenon<sup>6</sup>) for  $\sim 0.1$  keV, EUV lithography), soft x rays (e.g., ethanol,<sup>1</sup> ammonium hydroxide,<sup>7</sup> liquid nitrogen,<sup>8</sup> and argon<sup>9</sup> for  $\sim 1$  keV, microscopy and reflectometry), and hard x rays (copper solutions<sup>10</sup> for  $\sim 10$  keV, diffraction).

In this letter we extend the operation of EUV/soft x-ray laser-plasma sources to liquid-jet targets based on moderate-melting-temperature metals. This is of generic importance since laser plasmas on high- $Z$ , high-density targets have demonstrated very high conversion efficiencies. Furthermore, the low vapor pressure of these liquids practically eliminates the outgassing problem of liquefied inert gases such as xenon. Finally, the new range of target materials allows improved flexibility in spectral tailoring of the emission wavelengths. Here we focus on tin due to its current

interest as a source for  $\lambda \approx 13$  nm EUV lithography. Tin laser plasmas have significant potential for high conversion efficiency (CE) at 13 nm. Theoretical calculations<sup>11</sup> show that predominantly  $4d-4f$  transitions in a number of adjacent ion stages ( $\text{Sn}^{8+}-\text{Sn}^{13+}$ ) produce unresolved transition arrays (UTAs)<sup>12</sup> that are localized in this spectral area. Localization in combination with overlapping contributions from several ion stages create opportunities for high laser-plasma CE around 13 nm. In this letter we demonstrate a CE of 2.5% into ( $2\% \text{ BW} \times 2\pi \times \text{sr}$ ). Previous work on tin includes quantitative<sup>13</sup> as well as nonquantitative<sup>14-16</sup> measurements on nonregenerative bulk targets that reached up to 1.6% CE.<sup>13</sup> Regenerative laser-plasma tin targets have been demonstrated with droplets of tin solutions, resulting in lower tin density and lower CE ( $\sim 1\%$ ).<sup>17</sup> In addition, we present quantitative measurements of debris that indicate a significant debris problem. Outside the EUV/soft x-ray range, liquid-metal jets have been utilized for hard x-ray generation via femtosecond laser-plasma generation (low-melting-point gallium)<sup>18</sup> and via electron-beam-driven brehmsstrahlung generation (lead-tin alloys).<sup>19</sup>

Figure 1 depicts the experimental arrangement. The liquid-tin jet is generated by a liquid-metal-jet system consisting of a 0.15 l high-pressure tank, a sintered stainless-steel particle filter and a 75  $\mu\text{m}$  diam ruby pinhole nozzle.<sup>19</sup> The high-pressure tank is enclosed in an infrared (IR)-radiation heater capable of heating the tin (99.8%) up to  $>300$  °C. The liquid jet is injected into a vacuum chamber, which is evacuated to  $10^{-5}$  mbar by a 500 l/s turbodrag pump, by applying up to 200 bar of nitrogen driving pressure, resulting in jet speeds up to  $\sim 75$  m/s. The resulting positional stability of the jet is  $<5$   $\mu\text{m}$  at a distance of  $\sim 10$  mm from the nozzle orifice.

The plasma is generated by a 20 Hz Nd:YAG laser capable of delivering 300 mJ,  $\sim 5$  ns pulses at  $\lambda = 1064$  nm. By using a variable diffractive attenuator in the beam path, the pulse energy in the focus can be varied between 25 and 284 mJ without altering the temporal pulse shape or the beam profile. The beam is focused onto the liquid-metal jet to a minimum simulated full width at half maximum (FWHM) of

<sup>a)</sup>Electronic mail: per.jansson@biox.kth.se

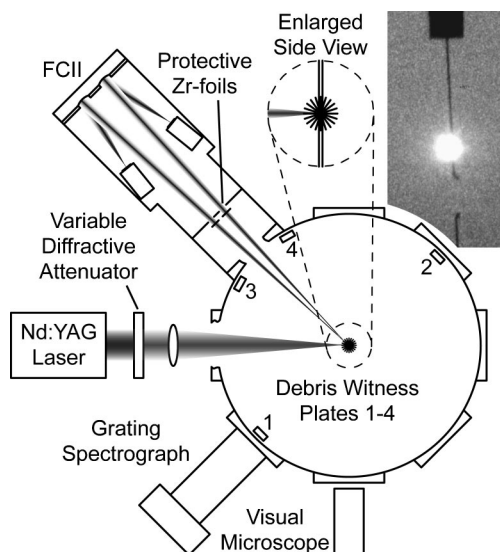


FIG. 1. Experimental arrangement of the liquid-metal-jet laser-plasma experiment. The photo shows a double-exposure of the jet and the plasma.

$\sim 17 \mu\text{m}$ . The focus can be moved in the horizontal plane with an accuracy of  $\sim 0.5 \mu\text{m}$ .

The jet and plasma are imaged at visible wavelength by a charge coupled device (CCD) detector attached to a long-working-distance  $12\times$  zoom microscope. A second 20 Hz,  $\sim 4$  ns pulsed frequency-doubled Nd:YAG laser is used to back illuminate the jet for time-resolved imaging. By synchronizing the illumination laser with the plasma-generating laser, enables the recording of doubly exposed images in which both the visual plasma and the gap created in the continuous jet can be observed (cf. Fig. 1). From these measurements we conclude that the present maximum operating frequency is approx 50 kHz.

Absolute measurements of the EUV flux are performed using a commercial instrument, Flying Circus II (FCII).<sup>20</sup> The actual FCII tool used in this experiment and its operation are described further in Ref. 21. FCII utilizes spherical narrow band multilayer mirrors at  $\lambda = 13.45$  nm in two parallel channels to focus the collected in-band EUV radiation through 200 nm thick zirconium filters onto diodes (AXUV 100). The calibrated equipment inside the UHV compatible FCII tool is shielded from the main chamber by an assembly with two Zr-filtered apertures to avoid contamination. By decreasing the radius of one aperture at the time and observing that the relative signal intensities of the FCII diodes do not change, errors due to spatial mismatch are avoided. The transmission of all Zr filters is obtained by using the filter wheel of the FCII, described in Ref. 21. During the tin experiments one of the apertures is fully closed except for short exposures during data collection, thus minimizing degradation of the filter and at the same time enabling monitoring of potential filter transmission loss of the continuously open aperture.

Spectra are recorded with a 1000 lines/mm freestanding transmission grating (Heidenhain) covered by a 200 nm Zr filter to remove visible light. The arrangement is equivalent to the one described in Ref. 22, except for the grating. An x-ray sensitive thinned, back-illuminated CCD is used as the detector. With the geometry used, resolution of  $\lambda/\Delta\lambda \approx 40$

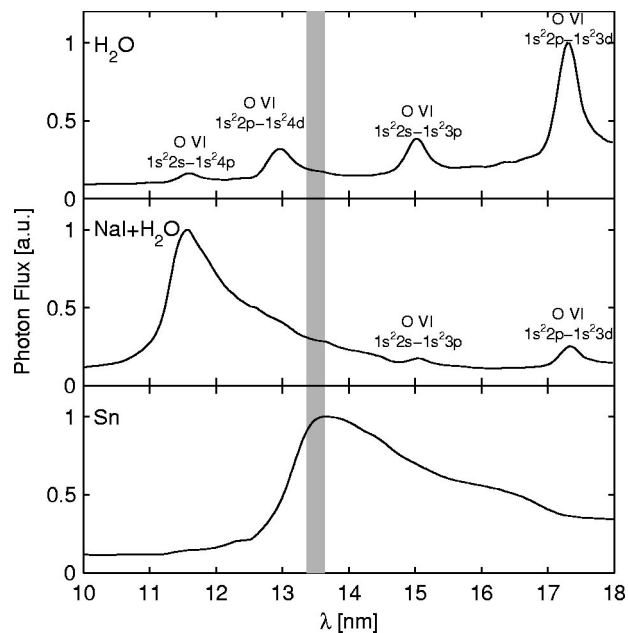


FIG. 2. Recorded spectra of laser-plasma-generated EUV emission from  $\text{H}_2\text{O}$ ,  $\text{NaI} + \text{H}_2\text{O}$ , and  $\text{Sn}$ . The shaded area depicts the 2% bandwidth region around  $\lambda = 13.5$  nm with high reflectivity of a Mo/Si multilayer system.

can be achieved in the 0–18 nm wavelength range assuming a source size of  $\sim 75 \mu\text{m}$ .

Due to the limited operating time of and significant emission of debris by the liquid-tin-jet system, calibration and alignment of the experimental arrangement were performed with liquid-jet targets of pure water and NaI dissolved in water. Figure 2 shows the spectra. The four strong oxygen emission lines from water were used for spectral calibration of the spectrograph. The broadband iodine emission from the NaI solution within the Mo/Si mirror bandwidth was used for geometrical alignment of the FCII tool and for transmission calibration of the Zr filters.

The lower part of Fig. 2 shows the spectrum from the liquid-tin-jet experiment. The spectrum was recorded at optimal CE conditions (discussed below) and it shows good agreement with that reported earlier.<sup>14–17</sup> Optimal CE was found by scanning the focus along the optical axis for seven different laser energies ranging from 25 to 284 mJ, thereby finding both the optimal spot size and intensity. CE was calculated from the FCII data assuming  $4\pi$  sr uniform emission from the plasma, negligible filter transmission degradation, and available calibration data for the FCII tool.<sup>21</sup> The maximum CE was  $2.5\% / (2\% \text{ BW} \times 2\pi \times \text{sr})$  at  $\lambda = 13.5$  nm for a pulse energy of 25 mJ and a focus intensity of  $\sim 5 \times 10^{11} \text{ W/cm}^2$ . The intensity is in good agreement with theoretical estimates predicting that  $\sim 2 \times 10^{11} \text{ W/cm}^2$  will produce an optimal plasma temperature of 33 eV (cf. Ref. 23). The pulse-to-pulse stability was  $\leq 1.5\%$  ( $1\sigma$ ). The CE compares favorably with that in Ref. 13 (1.6% on bulk tin) and that in Ref. 17 (1% on tin solutions). The CE numbers should also be compared with the present data on EUV liquid-jet xenon sources, 0.95%.<sup>24</sup> The higher tin CE is predominantly due to the better spectral match of Sn emission to the preferred 13.5 nm reflectivity maximum of the Mo/Si multilayer mirrors.<sup>11</sup>

Debris measurements were performed using partially

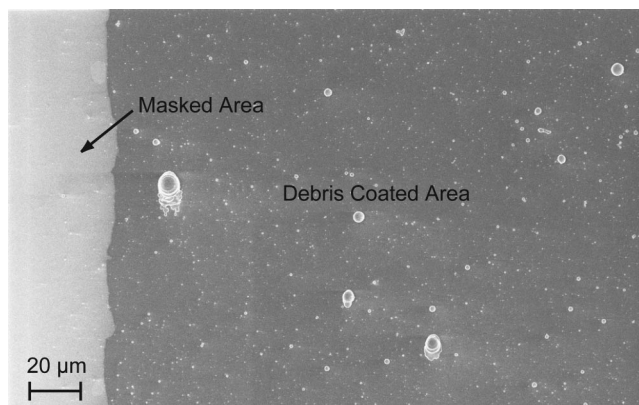


FIG. 3. SEM image of debris plate 3, where the particulate debris is clearly visible on the background due to ionic/atomic debris.

masked silicon wafer substrates as witness plates at four different positions 190 mm from the plasma (cf. Fig. 1). The substrates were shielded from the plasma by shutters until stable plasma operation was obtained. The witness plates were exposed for  $\sim 15$  min and analyzed by scanning electron microscopy (SEM) and a surface profilometer (KLA Tencor P-15). Examination of the four debris plates shows that debris emission is not distributed uniformly. Plates 1, 3, and 4 are sparsely covered with micrometer-sized particles on top of a thin background coating. The background coating of plates 3 and 4 is  $5.3 \pm 1$  nm ( $1\sigma$ ) thick. On these two plates there are also a few larger particles ranging from 10 to 50  $\mu\text{m}$  in diameter. A SEM image of plate 3 is shown in Fig. 3, where both the darker background coating and the particles described can be observed. Plate 2 is almost fully covered with the larger particles seen in plates 3 and 4, resulting in an average thickness of  $\sim 700$  nm.

Figure 1 shows that a  $\sim 1$  mm section of the jet is removed by each shot. Moreover, the debris plates indicate that only a fraction of the material removed is emitted as ions and atoms, while the rest is ejected as particles of different size, preferably in the forward direction. Assuming that the particulate debris is distributed in a  $2\pi$  sr solid angle, the theoretical layer thickness for plate 2 is  $\sim 720$  nm. Furthermore, if the ionic and atomic fraction of the ejected material is assumed to correspond to a 50  $\mu\text{m}$  section of the jet and is distributed in a  $4\pi$  sr solid angle, the theoretical layer thickness should be on the order of  $\sim 10$  nm. Although crude, these calculations show decent quantitative agreement with the experimental data. It can be argued that by using smaller-diameter jets or droplets, the amount of particulate debris can be limited, ultimately reducing the debris problem to only the ions and atoms. However, this fraction alone produces  $\sim 9 \times 10^{-7}$  g/pulse. In a future production-scale EUV lithography system operating at  $>7$  kHz with a 25% duty cycle,<sup>25</sup> this will result in an annual emission of  $\sim 50$  kg of ionic and atomic Sn, which will coat the collector mirrors positioned approx 10 cm from the source. In order to keep the loss in reflectivity of in-band EUV to  $<10\%$  (i.e.,  $<0.8$  nm Sn coating) a debris mitigation efficiency of  $\sim 10^8$  is therefore necessary. This will require a significant development effort since no such highly effective mitigation technique is presently available.

In summary, we have demonstrated the applicability of

liquid-metal jets as regenerative targets for stable laser-plasma generation of soft x rays and EUV radiation with high conversion efficiency. These targets allow high-repetition-rate operation ( $>50$  kHz) with low-vapor-pressure target materials. We demonstrated a very high CE into  $\lambda \approx 13$  nm using tin jets. The large debris production may prove to be a significant obstacle for practical utilization of the source in systems where long-term operation is necessary, making the present source primarily interesting for short-term experiments where debris is a minor issue.

The authors gratefully acknowledge support by the Swedish Science Research Council and the Swedish Agency for Innovation Systems.

- <sup>1</sup>L. Rymell and H. M. Hertz, *Opt. Commun.* **103**, 105 (1993).
- <sup>2</sup>L. Malmqvist, L. Rymell, M. Berglund, and H. M. Hertz, *Rev. Sci. Instrum.* **67**, 4150 (1996).
- <sup>3</sup>L. Rymell and H. M. Hertz, *Rev. Sci. Instrum.* **66**, 4916 (1995).
- <sup>4</sup>H. M. Hertz, L. Rymell, M. Berglund, and L. Malmqvist, *Proc. SPIE* **2523**, 88 (1995).
- <sup>5</sup>U. Vogt, H. Stiel, I. Will, P. V. Nickles, W. Sandner, M. Wieland, and T. Wilhein, *Appl. Phys. Lett.* **79**, 2336 (2001).
- <sup>6</sup>B. A. M. Hansson, L. Rymell, M. Berglund, and H. M. Hertz, *Microelectron. Eng.* **53**, 667 (2000).
- <sup>7</sup>L. Rymell, M. Berglund, and H. M. Hertz, *Appl. Phys. Lett.* **66**, 2625 (1995).
- <sup>8</sup>M. Berglund, L. Rymell, T. Wilhein, and H. M. Hertz, *Rev. Sci. Instrum.* **69**, 2361 (1998).
- <sup>9</sup>M. Wieland, T. Wilhein, M. Faubel, C. Eilert, M. Schmidt, and O. Sublemontier, *Appl. Phys. B: Lasers Opt.* **B72**, 591 (2001).
- <sup>10</sup>R. J. Tompkins, I. P. Mercer, M. Fettweis, C. J. Barnett, D. R. Klug, L. G. Porter, I. Clark, S. Jackson, P. Matousek, A. W. Parker, and M. Towrie, *Rev. Sci. Instrum.* **69**, 3113 (1998).
- <sup>11</sup>G. O'Sullivan, EUVL Source Workshop, Antwerp 2003; available at [www.semtech.org](http://www.semtech.org).
- <sup>12</sup>W. Svendsen and G. O'Sullivan, *Phys. Rev. A* **50**, 3710 (1994).
- <sup>13</sup>R. C. Spitzer, T. J. Orzechowski, D. W. Phillion, R. L. Kauffman, and C. Cerjan, *J. Appl. Phys.* **79**, 2251 (1996).
- <sup>14</sup>J. M. Bridges, C. L. Cromer, and T. J. Mc Illrath, *Appl. Opt.* **25**, 2208 (1986).
- <sup>15</sup>I. W. Choi, H. Daido, S. Yamagami, K. Nagai, T. Norimatsu, H. Takabe, M. Suzuki, T. Nakayama, and T. Matsui, *J. Opt. Soc. Am. B* **17**, 1616 (2000).
- <sup>16</sup>Y. Ueno, T. Aota, G. Niimi, D.-H. Lee, K. Nishigori, H. Yashiro, and T. Tomie, *Proc. SPIE* **5037**, 750 (2003).
- <sup>17</sup>C.-S. Koay, C. Keyser, K. Takenoshita, E. Fujiwara, M. Al-Rabban, M. C. Richardson, I. C. E. Turcu, H. Rieger, A. Stone, and J. H. Morris, *Proc. SPIE* **5037**, 801 (2003).
- <sup>18</sup>G. Korn, A. Thoss, H. Stiel, U. Vogt, M. Richardson, T. Elsaesser, and M. Faubel, *Opt. Lett.* **27**, 866 (2002).
- <sup>19</sup>O. Hemberg, M. Otendal, and H. M. Hertz, *Appl. Phys. Lett.* **83**, 1483 (2003).
- <sup>20</sup>R. Stuijk, R. C. Constantinescu, P. Hegeman, J. Jonkers, H. F. Fledderus, V. Banine, and F. Bijkerk, *Proc. SPIE* **4146**, 121 (2000).
- <sup>21</sup>B. A. Hansson, L. Rymell, M. Berglund, O. Hemberg, E. Janin, J. Thoresen, and H. M. Hertz, *Proc. SPIE* **4506**, 1 (2001).
- <sup>22</sup>T. Wilhein, S. Rehbein, D. Hambach, M. Berglund, L. Rymell, and H. M. Hertz, *Rev. Sci. Instrum.* **70**, 1694 (1999).
- <sup>23</sup>D. T. Attwood, *Soft X-Rays and Extreme Ultraviolet Radiation* (Cambridge University Press, Cambridge, 2000), Chap. 6.
- <sup>24</sup>B. A. M. Hansson, EUVL Source Workshop, Dallas (2002); available at [www.semtech.org](http://www.semtech.org).
- <sup>25</sup>H. Franken, Y. Watanabe, and K. Ota, EUVL Source Workshop, Antwerp 2003; available at [www.semtech.org](http://www.semtech.org).